Chapter 2

Experimental details

2. Experimental details

2.1. Procurement of raw materials and chemicals

All chemicals employed were of high purity analytical grade. Various chemicals used in the present investigations were: nitric acid, hydrochloric acid, sulphuric acid (Molychem India Pvt. Ltd., India and Fisher Scientific, India); n,n-Dimethyl acetamide (DMA) (Sisco Research Laboratories, India); Absolute ethanol (99.9%), acetone (Fisher Scientific, India); Sodium hydroxide (NaOH) (Qualigens fine chemicals, India); ammonia solution (Loba Chemie Pvt. Ltd., India); Acorga M5640 (Cytec India specialty chemicals & materials Pvt. Ltd., India); kerosene (Sigma-Aldrich). Additionally, ultrapure water (MilliQ, Millipore, 18.2 MΩ.cm at 25°C) was utilized for preparing solutions and washing samples. Waste printed circuit boards of computer motherboards of several makers were acquired from a regional vendor in Varanasi, India. Outdated cell phones like Nokia and Samsung GSM models were also gathered from nearby e-scrap vendors in Varanasi, India for this research.

2.2. Pre-processing of WPCBs

The external components mounted on the PCB namely resistors, capacitors, transistors, and diodes were mechanically separated with a hot air gun (*Stanley STXH 2000-IN*, Temperature <180°C) by melting the soldered joints after careful removal of coin-cell battery. The dismantled PCBs were then washed twice with hot water and acetone to eliminate dust, dirt or grease. Following this the neat WPCBs were shredded to 1 cm^2 size using a shear cutter. These shortened PCB pieces were dissolved in n,n-dimethyl acetamide (DMA) for dissolving the bonding resin from the surface of WPCBs, leading to dissolution of brominated epoxy resin (BER) and cracking of interlayers of glass fibre and metallic sheets (Verma et al., 2017a). The process of delamination was done for 180 min, at 140ºC temperature, with 3:10 solid to liquid ratio of WPCB shortened pieces and DMA at a

stirring speed of 300 rpm (Verma et al., 2017b). The passed down DMA was regenerated by distillation. The metallic layers were washed several times and dried at 80°C for 8 h. BER dissolution using organic solvent such as DMA helps in easy regeneration, and low effluent generation during delamination, thus reducing the toxicity levels during the recovery stage. Toxicity will be carried to the nanoparticle formation stage if it is not removed in the beginning. A graphical representation of the pre-processing is shown in *Figure 2.1*.

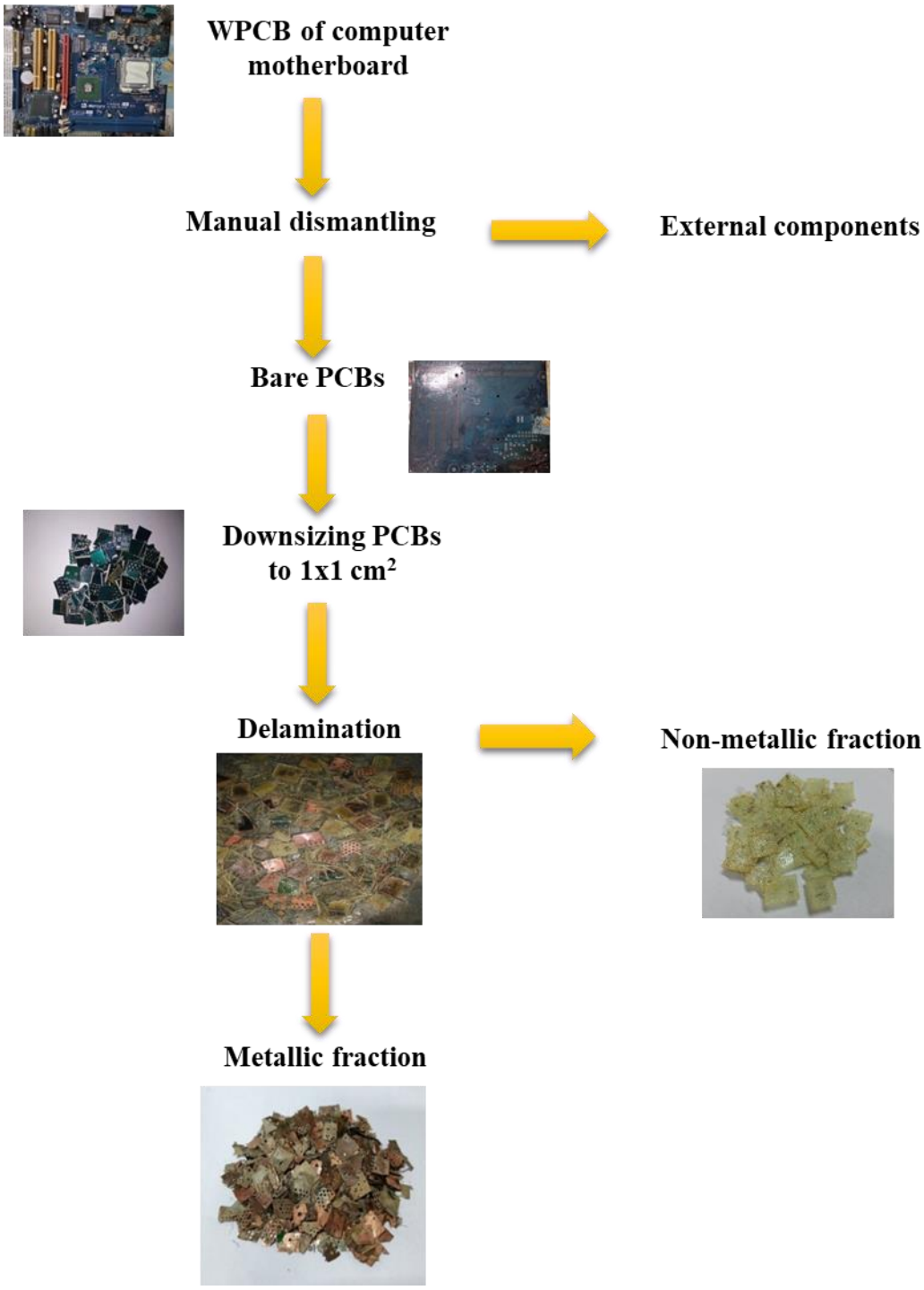

Figure 2.1 Pre-processing treatment of waste printed circuit boards

2.2.1. Estimation of composition in WPCBs

To estimate the composition of WPCBs of computer motherboards the downsized PCB pieces were initially pulverized to -1 mm size using a hammer mill make *Ikon Instruments*,

India. The inlet chute at the top of the mill was used for the feed and powder was collected from the bottom part of the mill. The maintained feed rate was 3 kg/h. The precise metal makeup of the ground WPCBs was established using Atomic Absorption Spectroscopy (AAS) through an *Elico SL 168* instrument. To do this, 2 grams of powder underwent dissolution in freshly prepared aqua regia, facilitating the digestion of metallic components. At first, aqua regia was introduced into a round-bottom flask with three necks and heated using a hot plate connected to a PID controller and thermocouple arrangement for precise temperature control. Upon reaching the preset temperature, the powdered sample was gradually introduced into the reaction vessel to facilitate digestion. A condenser was attached to the central neck to condense any vapors escaping the system. Continuous stirring was achieved using a PTFE-coated magnetic stirrer bar. Once all metallic components dissolved in the aqua regia, the undissolved non-metallic fraction was isolated via filtration using Whatman no. 42 filter paper. The filtered solution was diluted to a known volume by adding distilled water. A portion of the solution was extracted and further diluted with distilled water according to the working range of each element analyzed by AAS. The analysis revealed that the PCB powder contained 22.6 wt% copper, 2.9 wt% zinc, and other metals (11.48 wt%), while the rest comprised insoluble plastics and ceramics (63.02 wt%) as detailed in *Table 2.1.* Silver and gold are coated on the contacts of the components to prevent corrosion (Rao et al., 2020). Consequently, the milled powder displays a comparatively reduced metallic content for the leaching process. Simultaneously, the presence of PCBs hampers the leaching recovery rate owing to their structure, characterized by interlaced layers of metal cladding and non-metallic substrates (Havlik et al., 2010). Hence, the strategy involves separating these layers by dissolving the epoxy resin, functioning as a reinforcing agent, using an organic solvent.

Table 2.1 Chemical analysis of powder PCBs of computer motherboards

Element	Weight%
Cu	22.6
Ni	0.27
Zn	2.9
Al	4.2
Fe	3.4
Sn	2.24
Pb	1.2
Ag	0.16
Au	0.01
Total metal fraction	36.98
Others (Insoluble polymer and ceramic residues)	63.02

2.2.2. Analysis of composition of liberated metallic fraction

The metallic portion derived from the chemical pre-treatment underwent analysis using an X-ray diffractometer, specifically the Malvern Panalytical Empyrean model with a Pixel 3D detector. This analysis utilized Co-Kα radiation with a wavelength of 1.789 Å within a 2θ angular range spanning from 20º to 100º. The scanning speed was set at 0.5º/min with increments of 0.02º. Identification of phases was facilitated by referencing the JCPDS card number 10-1270. The XRD pattern reveals prominent copper peaks detected approximately at 50.7º, 59.3º, and 88.8º in the 2θ positions. Meanwhile, other peaks corresponding to trace metallic fractions were obscured by the intense copper peaks (see *Figure 2.2*).

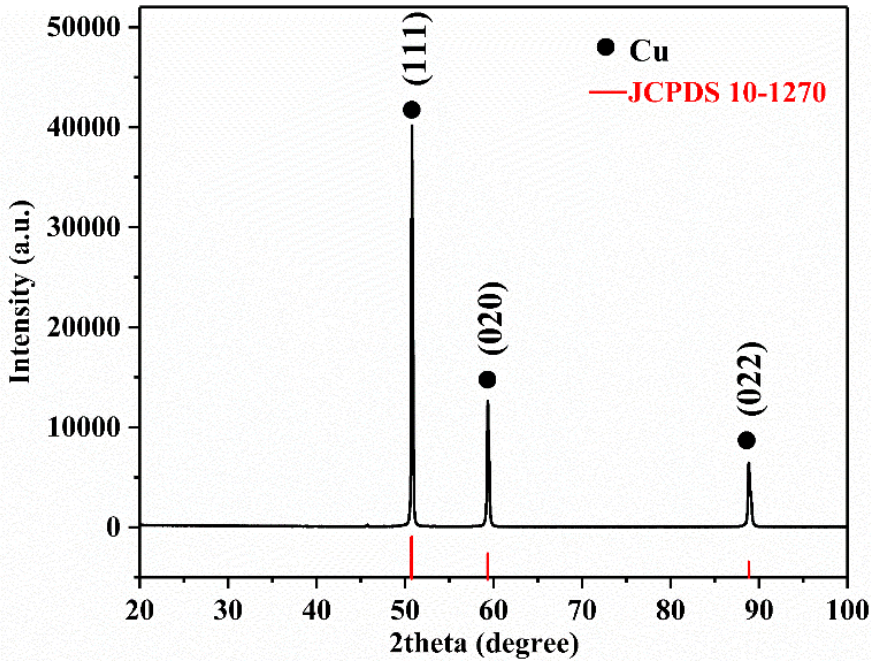

Figure 2.2 XRD analysis of metal clad

The accurate metal concentration of the metallic layer was obtained by dissolving the metallic clads in freshly prepared aqua regia ($HCl:HNO_3$ in 3:1 v/v ratio) at 50ºC for 2 h. The dissolved portion was filtered, accurately diluted with distilled water and analysed by AAS. It was found that the metallic fraction contained around 87.92 wt% copper, along with traces of nickel, zinc and silver (as listed in *Table 2.2*). Some plastics which did not separate from the metal foils during the pre-treatment stage formed the rest part of the composition.

Table 2.2 Chemical analysis of metallic fraction obtained from WPCBs of computer motherboards (after pretreatment)

Elements	Composition of WPCB after aqua regia leaching
Cu	87.92
Ni	0.15
Zn	0.57
Fe	-
Sn	-
Au	-
Ag	0.038
Others (Plastic and ceramic residues)	11.322

En dash (-) indicates not detected during analysis

2.3. Synthesis of copper oxide nanoparticles from copper-rich leach liquor of WPCBs of computer motherboards

The production of nano copper oxide involves three steps: leaching, precipitation, and calcination. The obtained liberated metal fraction was leached in nitric acid at optimized parameters with 3 M HNO_3, 30°C temperature, 2 h time period, 50 g/L pulp density and 500 rpm stirring speed. The leaching parameters were optimized by varying the nitric acid concentration between 1-3 M, temperature between 30-60ºC, pulp density between 25-100 g/L, and stirring speed between 100-500 rpm. 10 ml of the leach solution was used and either sodium hydroxide or ammonium hydroxide was utilized as the precipitation agent until the pH of the solution reached 8.5. After achieving the required pH, the solution was

further stirred for 1 h. Then the precipitates were centrifuged and washed several times with distilled water and ethanol to remove any impurities. The obtained blue powder was dried in vacuum oven at 60ºC overnight. Subsequently, the dried powder was calcined in a muffle furnace at 400ºC for 4 h to obtain a black powder. A graphical representation of the whole process is shown in *Figure 2.3*. Following this protocol, four black coloured powder samples namely N1, N2, N3, and N4 (as shown in *Figure 2.4*) were obtained and subject to further characterization techniques.

When 1 M NaOH solution is added to the leach liquor stirred at 30ºC, the sample obtained after precipitation, washing, drying, and calcination is termed as sample N1. Similarly, with 1 M NaOH solution and 60ºC reaction temperature, sample N2 is obtained. With 2 M NaOH solution and 30ºC reaction temperature, sample N3 is obtained. With 2 M ammonia solution (as precipitating agent) and 60ºC mixing temperature, sample N4 is obtained. When 1 M ammonia solution was used as a precipitating agent, no visible precipitation was observed at 30ºC reaction temperature. Ammonia forms strong coordination compounds with transition metals such as Cu, Ni, Zn and others (Etschmann et al., 2011). These are highly soluble and exist as stable complexes in aqueous solution. In the case of Cu, ammonia (NH_3) complexes with cuprous or cupric ions forming $Cu(NH_3)_4^{2+}$, generating an increase in solubility between pH 8.5 to 10.5. This tetra-amine-cupric complex formed with increasing pH is stable and hence does not precipitate above pH 8 (Velásquez-Yévenes and Ram, 2022). So with the use of ammonia as precipitant we were not able to harvest any precipitates.

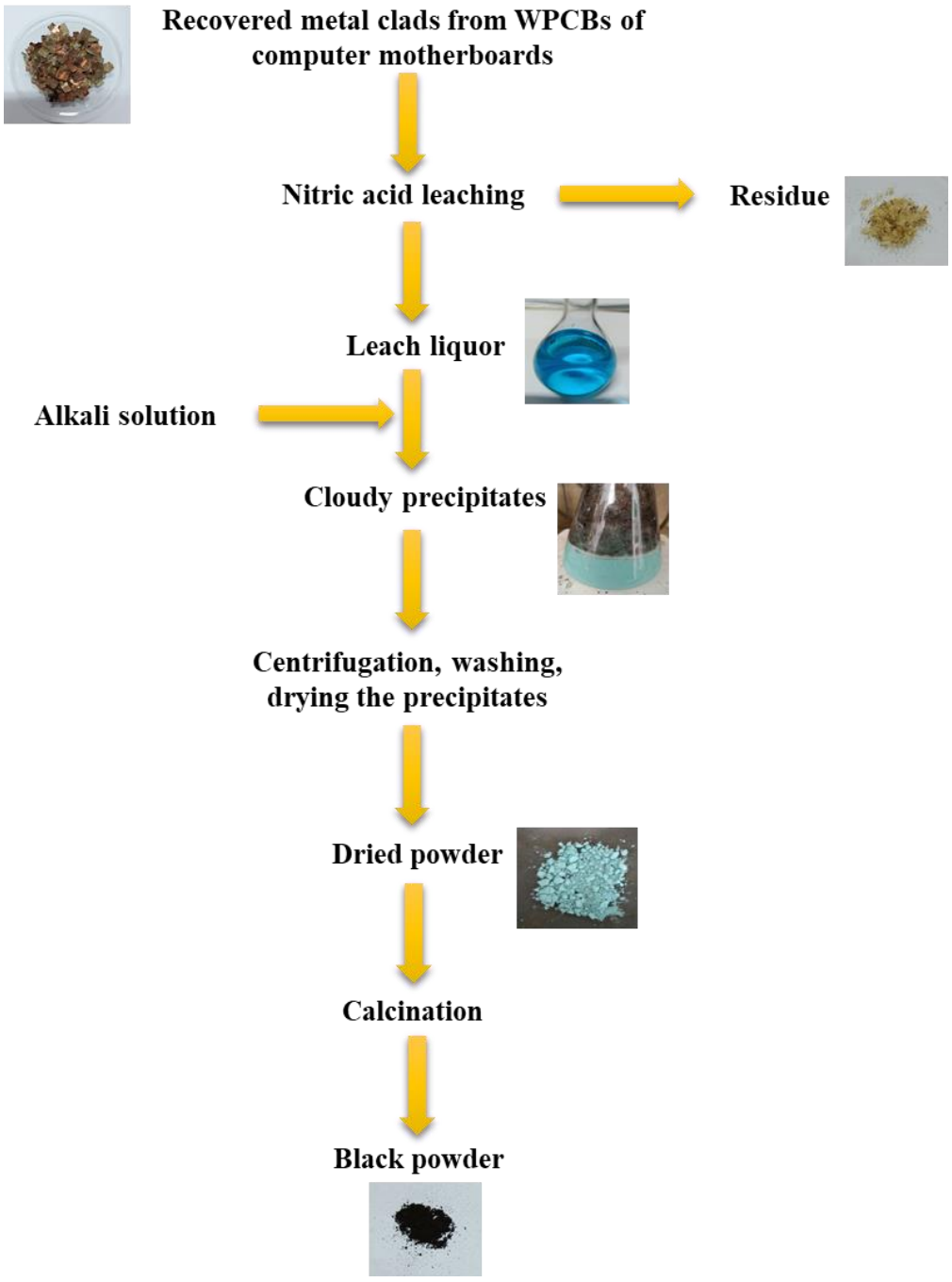

Figure 2.3 Graphical representation of copper dissolution from WPCBs and synthesis of CuO nanoparticles

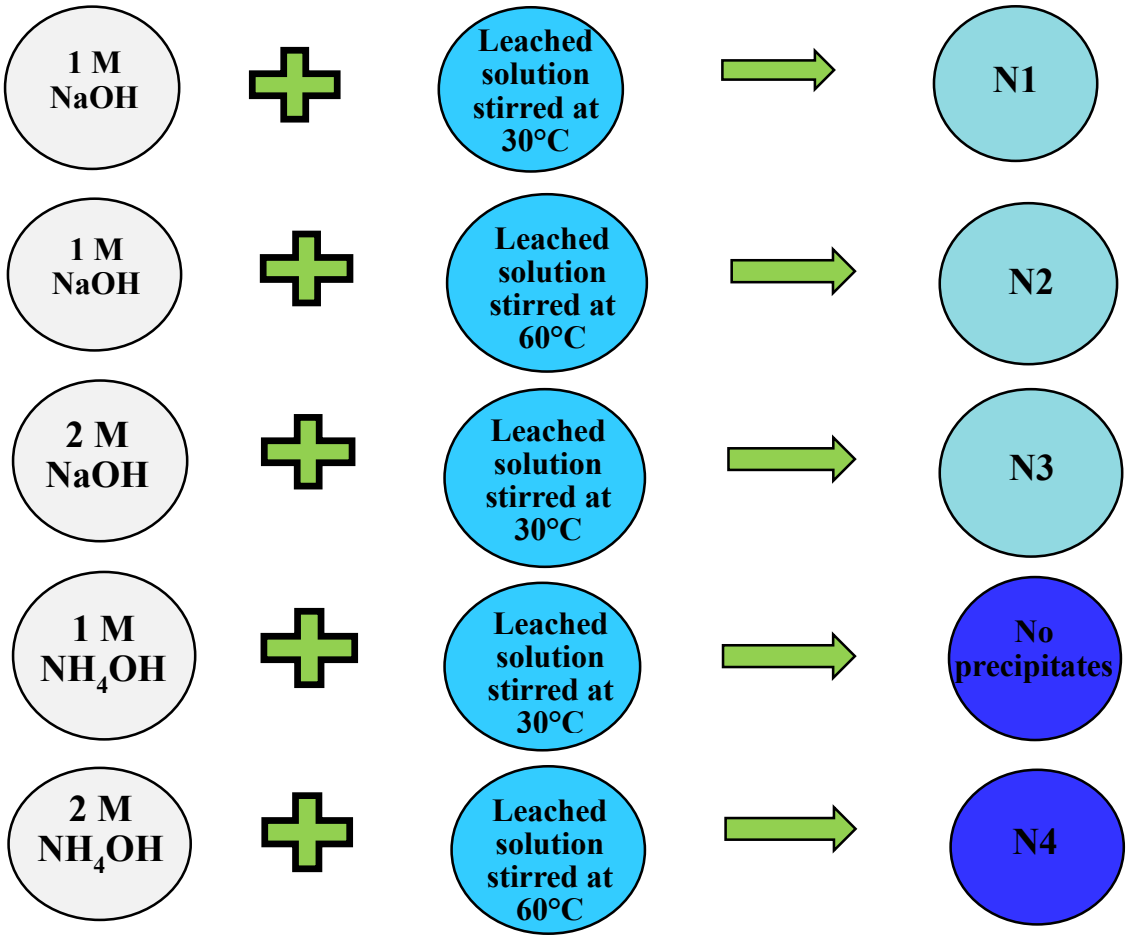

Figure 2.4 Graphical representation of all the samples obtained by this synthesis route

2.4. Application of CuO nanoparticles: Photocatalytic property measurements by evaluating the degradation of textile dyes Congo red and Methylene blue

The as-recovered nanoproducts are further explored as potential photocatalysts for the degradation of Congo Red (CR) and Methylene Blue (MB) textile dyes in presence of visible light. According to Beer-Lambert Law (Raja and Barron, 2024), the transmittance and absorbance (A) (arbitrary units) of a certain substance is proportional to its concentration in solution (M) (C) *(Eq. (2.1)*),

i.e. A α C i.e. A = εbC (2.1)

where ε is the molar absorptivity of the compound or molecule in solution (M-1cm-1), b is the path length of the cuvette or sample holder (usually 1 cm). So hence forth absorbance will be denoted as concentration.

2.4.1. Degradation of Congo red

The photocatalytic activity of the as-recovered copper oxide nanoparticle samples were evaluated for degradation of Congo Red (CR). 1 ml distilled water, 1 ml of CR aqueous solution (40 ppm) and 50 µl dispersion nanoparticle solution (1 mg CuO was dispersed in 2 ml distilled water) were mixed together in a 4 ml quartz cuvette. The mixture was stirred in a dark environment for 25 min to ensure complete adsorption-desorption equilibrium. Then the mixture was kept in a home-made photocatalytic chamber for visible light irradiation. Four Philips cool LED bulbs were used inside the chamber as visible light source. The UV-visible absorption spectrum of the reaction mixture was recorded at set time intervals. Congo red degradation was examined using UV-visible spectroscopic technique. The characteristic absorption peak of congo red observed at wavelength of 497 nm, related with an azo group (Rajeswari et al., 2018), slowly decreased with increase in

irradiation time and at last, the absorption peak disappeared and the color of the Congo red solution turned from red to colorless. The percent degradation of dye was calculated using *Eq. (2.2)*,

$$\%Degradation = (\frac{C_0 - C}{C_0})x\ 100 \qquad (2.2)$$

where C_0 is the initial dye concentration, C is the dye concentration at time t after exposure to visible irradiation.

2.4.2. Degradation of Methylene blue

To evaluate the degradation of Methylene Blue (MB), 1 ml distilled water, 200 µl of MB aqueous solution (40 ppm), and 100 µl dispersion nanoparticle solution (1.6 mg CuO was dispersed in 3 ml distilled water) were mixed together in a 4 ml quartz cuvette. The mixture was stirred in a dark environment for 25 min to ensure complete adsorption-desorption equilibrium. Then the mixture was kept in a home-made photocatalytic chamber for visible light irradiation. Four Philips cool LED bulbs were used inside the chamber as a visible light source. The UV-visible absorption spectrum of the reaction mixture was recorded at set time intervals. Degradation of MB was monitored using *Eq. (2.2)* by measuring the absorbance of MB at 664 nm wavelength (Blažeka et al., 2020).

2.5. Synthesis of $Cu(OH)_2$/CuO hybrid nanostructures and CuO nanoparticles from strip solution of mobile phone PCBs

2.5.1. Preparation of copper-rich strip solution from obsolete mobile phone PCBs

The strip solution obtained from PCBs used in mobile phones was chosen as primary material in the experiments. Specifics of the process for preparing the copper strip solution from PCBs were published in a previous study as explained in *Figure 2.5* (Rao et al., 2021). Briefly, metallic clads liberated from delaminated PCBs (containing 84 wt% copper) were

dissolved in 3 M HNO_3 at 30°C, 2 h period, 50 g/L pulp density, 500 rpm agitation to obtain a base metal rich solution. Copper was selectively separated from this leachant by liquid-liquid extraction with 30 vol% ACORGA M5640 mixed with kerosene (800 g/L) as extractant at 20°C temperature, 2 pH, 1:1 organic to aqueous phase ration, 1 h agitation time, followed by stripping with 4 M sulfuric acid maintained at pH 0.9. This purified stripped solution contains 99.9% copper, with small amounts of zinc (0.05%) and lead (0.02%).

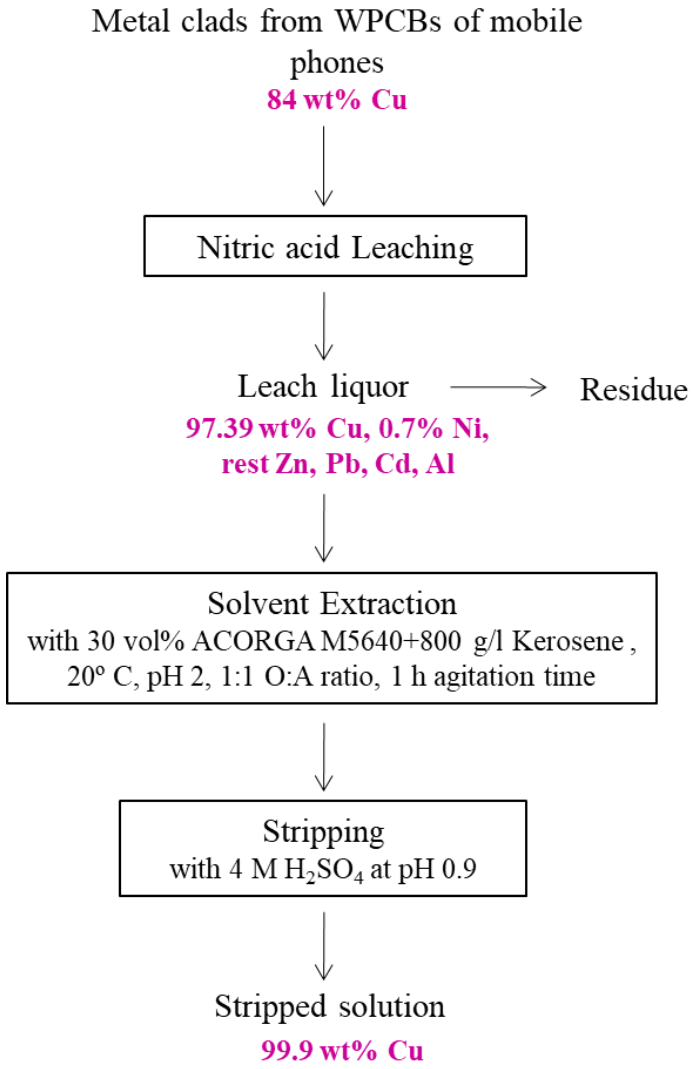

Figure 2.5 Process of obtaining copper strip solution from mobile phone PCBs (Rao et al., 2021)

2.5.2. Synthesis of $Cu(OH)_2$/CuO hybrid nanostructures and CuO nanoparticles from strip solution of mobile phone PCBs

The synthesis of nanostructures of CuO were carried out via a simple precipitation route using Cu-strip solution and NaOH solution at relatively low temperatures of 70 and 80°C. 1 M NaOH solution was introduced in drops to the Cu-precursor solution under persistent agitation till pH of the solution reached 8.5. The solution was further agitated magnetically for 1 h. The reaction mixture was shifted into a scotch-durant bottle and the cover of the bottle was tightly closed. This bottle was subjected to an oven at 70°C for a duration of 24 h. The supernatant solution was removed. Black coloured precipitates were harvested, washed repeatedly with distilled water and methanol by centrifugation to exterminate impurities, and dried at 50°C overnight. This sample was named P1. Another powder sample was prepared similarly by maintaining the scotch-durant bottle in oven at 80°C for 24 h. This powder was named P2. The illustrative depiction of the process followed is given in *Figure 2.6*. Umar et al., 2021 reported the formation of ultrathin leaf-shaped CuO nanosheets and investigated its application as a hydrogen sulfide gas sensor. They used copper (II) nitrate trihydrate as chemical precursor and NaOH as precipitant until pH of solution reached 11. Then the reaction mixture was transferred in scotch-durant bottle and placed in oven and maintained at 70ºC temperature for 24 h (Umar et al., 2021). In chapter 4 we had worked with 60ºC temperature. So we wanted to understand how playing with the temperature further i.e. increasing it to 70º and 80ºC will affect the morphology and properties of the CuO nanomaterial. We further investigated its photocatalytic property by assessing the degradation of rhodamine blue dye in the presence of visible light radiation.

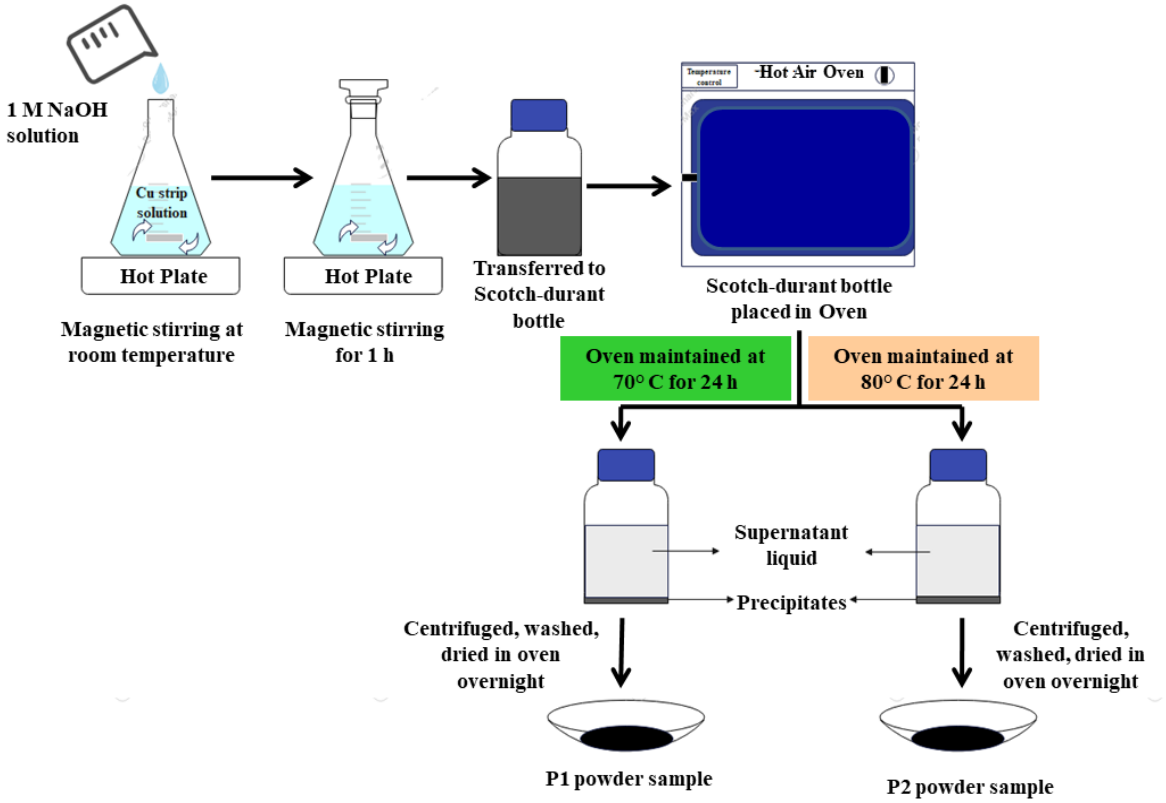

Figure 2.6 Graphical illustration of the synthesis of CuO-based nanostructures from Cu strip solution of PCBs

2.6. Assessment of photocatalytic property of $Cu(OH)_2$/CuO hybrid nanostructures and CuO nanoparticles: Degradation of Rhodamine blue

To assess the photocatalytic effectiveness of P1 and P2 samples, degradation of Rhodamine Blue (RhB) under visible light was examined. To a mixture of 2 ml distilled water, 200 µl RhB solution in water (4 ppm), 50 µl of nanoparticle dispersed solution was added in a cuvette of 4 ml volume. The nanoparticle dispersion solution was prepared by adding 2.1 mg solid catalyst to 3 ml distilled water. The solution was first stirred in dark for 15 minutes to attain complete equilibrium. Next, the solution was exposed to light for the specific duration of the trial. Four LED bulbs of the make Philips were employed as a source of visible light in the chamber. The solution was examined with a UV-visible

spectrophotometer at defined time frames to monitor the degradation of RhB. The absorbance of RhB dye at 553 nm was calculated to observe the degradation.

2.7. Material Characterization techniques

The high added-value products (HAVPs) are analysed using different characterization methods to get insight into their physicochemical properties such as particle size, morphology, structure, composition, and phases. These include X-ray diffraction, Fourier transform infrared radiation, Scanning electron microscopy, Transmission electron microscopy, X-ray photoelectron spectroscopy, Brunauer-Emmett-Teller, Atomic absorption spectroscopy, and others (*Table 2.3*).

2.7.1. Atomic Absorption Spectroscopy (AAS)

The AAS technique involves investigating how neutral atoms in a gaseous state absorb radiant energy, typically in the visible and UV spectra. In this method, the metal ions under examination are reduced to their elemental form, vaporized, and exposed to a beam of radiation emitted by an external light source. To generate a flame, both an oxidant gas (such as air or nitrous oxide) and a fuel gas (like acetylene) are necessary. Typically, a hollow cathode lamp specific to the element of interest is utilized to provide light across various wavelengths. To calibrate the AAS instrument, the absorption of solutions containing known quantities of elements is measured. The concentration of these elements is then determined using a calibration curve, which establishes the relationship between absorbance and concentration, following Beer-Lambert law as shown in *Eq. (2.3),*

$$A = \lambda * b * c \qquad (2.3)$$

where A is absorbance, λ is wavelength at which absorption is observed, b is length of light path, c is concentration.

The analysis was carried out in an Elico SL 168 instrument. Samples dissolved in distilled water were drawn into a PTFE (Teflon) capillary tube at a rate of 5.0 mL min^{-1}, then directed into a pneumatic nebulizer and a spray chamber made of glass beads and high density polyethylene (HDPE). For the aqueous samples, air-acetylene flame conditions were established: acetylene (C_2H_2) served as the fuel at a pressure of 15 psi, while continuous dry air acted as the oxidant at an input pressure of 50 psi. The flow rates for the fuel and oxidant were set at 3 and 2 L min^{-1}, respectively. Standards for AAS analysis were sourced from Sigma-Aldrich.

2.7.2. Powder X-Ray Diffraction (XRD)

X-ray powder diffraction stands as a fundamental analytical method employed for identifying phases and analyzing the structure and composition of (unknown) crystalline nanoparticles. It relies on the constructive interference between monochromatic X-rays and a crystalline sample. Because X-rays possess wavelengths within the interatomic spacing range of a crystalline solid, they diffract in specific directions according to Bragg's law. The resulting diffraction pattern, characterized by the intensities and positions of diffraction effects, yields crucial insights into structure identification. It is a non-destructive process because the solid samples can be recovered after the analysis. Powder x-ray diffraction pattern of the sample was done in Malvern Panalytical Empyrean instrument with pixcel 3D detector attachment using Co Kα (λ=1.789 Å) radiation in an angular range of 30-100° at a scanning rate of 2° min^{-1}, and at step size of 0.01. The structural assignments were done in agreement with the JCPDS powder datasets to identify the phases formed. The lattice parameter was calculated with the help of the following Bragg's equation (Pope, 1997) (*Eq. (2.4)*),

$$n\lambda = 2dsin\theta \quad (2.4)$$

where the order of reflection is assigned as n, λ is the wavelength of incident X-ray radiation, and θ is the Bragg angle between the incident light and the crystallographic plane.

2.7.3. Fourier Transform Infrared Radiation (FTIR)

FTIR employs an interferometer to modulate light intensity across different wavelengths using audio frequencies. A beam splitter divides light from an infrared source into two paths, recombining them to create a modulated optical path difference. This recombined beam undergoes constructive and destructive interference based on the instantaneous optical path difference. The most common method is the Michelson interferometer. Light from each path is reflected by fixed and moving mirrors, with constructive interference occurring when the optical paths are equal. Any deviation results in constructive or destructive interference depending on the phase relationship. The infrared radiation spectrum of the synthesized material was recorded employing a Thermo Scientific Nicolet iS5 FTIR Spectrometer under attenuated total reflectance (ATR) conditions set in the range of 400-4000 cm^{-1}.

2.7.4. Scanning Electron Microscope (SEM)

SEM imaging and Energy Dispersive Spectroscopy (EDS), widely used surface analytical techniques, were undertaken for nanoparticle imaging and analyzing the elemental composition of the samples. The samples were prepared following the standard sample protocol for powder nanoparticle

samples. First, a small amount of powder sample was properly spread on carbon tape. The excess sample was removed by a small air duster. The prepared carbon tape was put in the SEM instrument for imaging. The morphology was examined by high resolution scanning electron microscope (HR-SEM) of the build FEI Nova Nano SEM 450, and energy-dispersive x-ray (EDX) analysis was carried out using Team of Pegasus Integrated EDS-EBSD.

2.7.5. Transmission Electron Microscopy (TEM)

TEM tool is very useful for nanoscale imaging. Further, the high-resolution images give the structural information of the specific crystalline phases (Smith, 2015). It can also analyze the nanoparticle shapes and sizes. This thesis utilized a standard method for TEM sample preparation. First, the nanoparticles (of the concerned sample) were dispersed in ethanol by proper sonication and dilution. Then, one drop of the re dispersed sample was transferred to the TEM grid (carbon coated Cu grid with 400 mesh size). The sample grid was dried in an oven at 50°C overnight. FEI Technai G-2 electron microscope using 200 kV accelerating voltage examined the prepared TEM sample grid. The images were collected from the different regions of the grid. The images give shapes and average particle sizes. The average particle sizes and fringes d-spacing were calculated using ImageJ software.

2.7.6. X-ray photoelectron spectroscopy (XPS)

XPS is a quantitative analytical technique that measures the chemical state of the elements present in the material. When X-rays fall on the material, it causes the photoelectric effect. The ejected electrons move with certain kinetic energies that are analyzed by a detector. The binding energies are derived from these kinetic energies. Notably, the binding energy of an element of a particular oxidation state is specific. Sample preparation for the XPS measurement followed a standard protocol. First, the powder sample was dispersed in ethanol and then dropped on a square-shaped small glass slide. The treated glass slide was then dried in a hot air oven. The glass slide with the sample thin film was subjected to XPS measurements. All the XPS measurements were carried out on the K-alpha XPS instrument (Thermo Fisher Scientific).

2.7.7. UV-visible diffuse reflectance spectroscopy (UV- DRS)

The UV-DRS was utilized to measure the bandgap of the synthesized photocatalysts. The UV-2600 spectrophotometer (Shimadzu Company) recorded the reflectance spectra of samples. Then, the absorbance data was acquired from the reflectance data using the Kubelka-Munk method (Molenaar and Zijp, 1999; Yang and Kruse, 2004). The absorbance data generated the Tauc plots by the following relation (*Eq. (2.5)*):

$$(\alpha h\nu)^{1/n} = (h\nu - E_g) \quad (2.5)$$

Here, α is the molar absorption coefficient, E_g and ν are the material's bandgap and frequency of light. The x-axis intercept of the tangent to the linear part of the plot (1/n vs. hυ) gives the optical band gap (E_g) value of the photocatalyst. The n value governs the nature of the optical bandgap. For direct and indirect bandgap, the value of n is ½ and 2, respectively.

2.7.8. UV-Visible spectroscopy

UV-visible absorption spectroscopy is an analytical technique that measures light absorbance in the ultraviolet (UV) and visible regions of the electromagnetic spectrum. Light can be absorbed, transmitted, and reflected when it passes through the sample solution. Light absorption photo-excites electrons in a molecule by n- π*, π- π*, n- σ* (where the symbols indicate non-bonding orbital (n), bonding π-orbital (π), anti-bonding π–orbital (π*) or anti-bonding σ-orbital (σ*)) electronic excitations. The functional groups in the molecule cause a specific absorption, which is detected by a UV-vis detector and recorded as a UV-vis absorbance spectrum. The Agilent Cary 60 spectrophotometer generates all UV-visible spectra of the samples. The diluted sample solution was taken in a cuvette of 1 cm path length and put in the spectrometer's sample holder slot. Note that the solvent was used for baseline correction.

2.7.9. Brunauer-Emmett-Teller (BET) method

BELLSORP MAX II & BELCAT-II (MicrotracBEL Corp.) were used to determine surface area and pore size distribution in the powder sample by recording the N_2 adsorption/desorption isotherms at 77.4 K.

Gas sorption is the characterization method mainly used to determine the surface area of different materials. Surface area is usually determined by the BET method. First the sample is outgassed under a vacuum to remove moisture, gases, and other impurities. After this, the sample system is kept at the boiling point of the gas (N_2 at 77 K, Ar at 87 K) during the analysis. While the system is under vacuum, the sample is cooled to cryogenic temperature. Afterward, the adsorbent gas is introduced to the sample tube. After each dosing, the pressure equilibrium is reached, and then the amount of adsorbed gas is calculated. This step is repeated over a wide range of relative pressures, and adsorption isotherms are obtained as a result. Adsorption isotherm offers valuable information such as the amount of gas required to form a monolayer (one molecule thick) at the surfaces of the porous sample from which the surface area is calculated. Depending on the type of adsorption isotherm, the material is classified as micro, meso, or macroporous material (Horvat et al., 2022).

The BET theory was developed by Stephen Brunauer, Paul Emmett, and Edward Teller in 1938 (Raja and Barron, 2024). The first letter of each publisher's surname was taken to name this theory. The BET theory was an extension of the Langmuir theory, developed by Irving Langmuir in 1916. The Langmuir theory relates the monolayer adsorption of gas molecules, also called adsorbates, onto a solid surface to the gas pressure of a medium above the solid surface at a fixed temperature to

$$\theta = \frac{\alpha.P}{1+(\alpha.P)} \qquad (2.6)$$

where θ is the fractional cover of the surface, P is the gas pressure and α is a constant.

The Langmuir theory is based on the following assumptions:

- All surface sites have the same adsorption energy for the adsorbate (argon, krypton or nitrogen gas). The surface site is defined as the area on the sample where one molecule can adsorb onto.
- Adsorption of the solvent at one site occurs independently of adsorption at neighboring sites.
- Activity of adsorbate is directly proportional to its concentration.
- Adsorbates form a monolayer.
- Each active site can be occupied only by one particle.

The Langmuir theory has a few flaws that are addressed by the BET theory. The BET theory extends the Langmuir theory to multilayer adsorption with three additional assumptions:

- Gas molecules will physically adsorb on a solid in layers infinitely.
- The different adsorption layers do not interact.
- The theory can be applied to each layer.

The BET Equation (*Eq. (2.7)*) uses the information from the isotherm to determine the surface area of the sample:

$$\frac{1}{X[(\frac{P_0}{P})-1]} = \frac{1}{X_m C} + \frac{C-1}{X_m C}(\frac{P}{P_0}) \qquad (2.7)$$

where X is the weight of nitrogen adsorbed at a given relative pressure (P/Po), X_m is monolayer capacity, which is the volume of gas adsorbed at standard temperature and pressure (STP) [STP is defined as 273 K and 1 atm, C is BET constant.

Total surface area S_t can be calculated with *Eq. (2.8)*,

$$S_T = \frac{X_m N_A A}{M_v} \qquad (2.8)$$

where N_A is Avogadro's number, A is the cross sectional area of the adsorbate and equals 0.162 nm^2 for an absorbed nitrogen molecule, and M_v is the molar volume and equals 22414 mL.

The BET method of measuring specific surface area is based on the determination of the amount of gas that is adsorbed on the surface of the sample. The specific surface area (m^2/g) determined by this method (*Eq. (2.9)*) includes the external as well as internal (pores) surface area (Sydney and Hoganas, 2018).

BET specific surface area, $S_{BET} = \frac{Total\ surface\ area}{Mass\ of\ sample} = \frac{n_m L \sigma_m}{V_0 m}$ (2.9)

where, L is Avogadro's constant, σ_m is molecular cross-sectional area of adsorptive, m is sample mass, V_0 is molar gas volume of adsorptive at STP (Raja and Barron, 2024).

Table 2.3 List of characterization methods involved in the study of value-added products

Characterization technique	Parameters studied
Atomic Absorption Spectroscopy (AAS)	Analysis of concentration of elements in solution
X-ray diffraction (XRD)	Determination of phase, structure, crystallite size
Fourier transform infrared spectroscopy (FTIR)	Identification of functional group associated with NPs, chemical bonding
Scanning electron microscopy (SEM)	Surface morphology of NPs, crystalline structure
Energy dispersive x-ray (EDX)	Identify the composition and concentration of different elements present in a specific sample; purity
Transmission electron microscopy (TEM)	Morphology, size, and shape of NPs
X-ray photoelectron spectroscopy (XPS)	Provides quantitative and chemical state information of surface (upto 5 nm); valence band structure; elemental identification; binding energy
Brunauer-Emmett-Teller (BET)	Specific surface area
UV-visible (UV-Vis) spectroscopy	To confirm the synthesis of NPs in terms of structure, size, aggregation, absorption measurements